

# The Critical Coupling Likelihood Method: A new approach for seamless integration of environmental and operating conditions of gravitational wave detectors into gravitational wave searches.

Cesar A. Costa <sup>1</sup> and Cristina V. Torres <sup>2</sup>

<sup>1</sup>Louisiana State University

<sup>2</sup>LIGO Livingston Observatory

E-mail: [cesar.costa@ligo.org](mailto:cesar.costa@ligo.org)

[cristina.torres@ligo.org](mailto:cristina.torres@ligo.org)

**Abstract.** As part of the current LIGO search for gravitational waves (GWs) we find ourselves trying to determine if and when noise is coupling into the instrument. The Critical Coupling Likelihood (CCL) method has been developed to directly fold information about the potential influence of instrument noise sources into GW search efforts. By using the CCL functions of uncoupled (background) and coupled (foreground) instrumental noise sources, CCL should be able to identify undesirable coupled instrumental noise from potential GW candidates. Our preliminary results show that CCL can associate up to  $\sim 80\%$  of observed artifacts with  $SNR \geq 8$ , to local noise sources. That reduces the duty cycle of the instrument by  $\lesssim 15\%$ . An approach like CCL will become increasingly important as we move into the Advanced LIGO era, going from a first GW detection to gravitational wave astronomy.

PACS numbers: 04.80.Nn, 95.55.Ym, 07.60.Ly

## 1. Introduction

Gravitational waves (GWs) are perturbations on the local space-time metric which are associated with distant astrophysical phenomena. According to General Relativity, these perturbations travel at the speed of light and are generated by astronomical scale masses with time varying quadrupolar and higher moments. The main goal of the Laser Interferometric Gravitational Wave Observatories (LIGO) is to detect GWs and use this information to study the astrophysics associated with those sources [1].

The LIGO observatories are now undergoing a major upgrade. This upgrade will increase the instruments sensitivity, extending their observational range from the current  $\sim 20\text{Mpc}$  to  $\sim 100\text{Mpc}$  [2]. This change in the observational volume should increase the expected observable rate of GW signals. Using the network of GW detectors, one can expect detection rates to improve from  $1/50\text{yr}^{-1}$  to  $40\text{yr}^{-1}$  [3, 4]. In order to achieve such sensitivity, LIGO instruments will be completely refitted with advanced components and control systems. This new configuration is called Advanced LIGO (aLIGO). During the aLIGO operational era, the first GW detection will mark the beginning of gravitational wave astronomy.

For initial LIGO, searches for GWs were hindered by computational costs, human resource costs, and concentrated instrumental knowledge. But as LIGO has matured many of these limiting factors have been addressed. However human instrumental expertise and commissioning knowledge remains the most scarce resource for conducting GW searches. In all previous observing epochs, LIGO's search efforts have relied on post-facto human study of potential signals and their characteristics, a process known as *followups*. The followup is a human resource intensive stage in a GW search and it continues to be a limiting factor on how quickly a search is completed. This tradition of following up individual events in GW searches will be difficult to sustain in an era of GW astronomy, where regular detections should be common place [5].

Although the first GW detection will be heavily reviewed using the traditional followup style, all subsequent detections should integrate followup procedures into the search process. In order to effectively remove this human resource intensive activity, information about instrumental operating conditions must successfully be integrated into a GW search. The state of the instrument, and hence the data quality (DQ) have a significant impact on the effectiveness of LIGO's GW searches. In this paper, we are proposing a method to quantify instrumental operating conditions and discuss how this information could be integrated into future GW searches. Our method is a significant departure from LIGO's current style of integrating instrumental information (Data Quality - DQ) [6].

Understanding non-Gaussian noise sources is preponderant to isolate them during the search process without compromising the instrument duty cycle. These transient noise sources are typically the result of a local external influence on the instrument. These transient noise sources, can lead to GW candidates which are false and in reality an artifact resulting from some local disturbance. In order to uncover the sources of these coupled artifacts in LIGO data there are a large number of external sensors, which LIGO refers to as instrumental and environmental monitors.

LIGO records information about the physical operating environment and also information about the control subsystems of the interferometer. This information is used to determine if a GW candidate is or is not an artifact produced by a glitch in the system. In order to accomplish this, each of the sensors are analyzed to identify

departures from their nominal behavior. This approach is currently how candidates resulting from glitches are identified and discarded at the end of a GW search.

We propose to improve GW searches by introducing our method, the **Critical Coupling Likelihood (CCL) Test**. This test is intended to integrate information about the instrument condition, and its environment directly into a search. This integrated information will be used to determine the significance level of a potential GW candidate. Also such integration into the early phase of a GW search should remove the need for performing traditional candidate followups, as was done in previous LIGO analysis.

## 2. The Critical Coupling Likelihood

CCL is a technique intended to quantitatively identify as many avenues of environmental to instrumental coupling as possible. This statistical method can identify coupling measurements independently of any particular assumed transfer function. As many other methods, this technique is also based on time coincidence between event pairs from preselected data streams. Normally, on LIGO Detector Characterization Methods, this pairing is done by using the GW data stream (GW channel) and an auxiliary sensor data stream (sensor channel). What differs CCL from other methods is its capability of distinguishing real time coincidence (coupling) from accidental coincidences.

It is well known that all instruments have random fluctuations due to inherent noise, which if Gaussian in nature is uncorrelated between a pair of input data channels. Regardless of the inherent noise of both channels, the CCL test is designed to be insensitive to Gaussian components of that well behaved random noise.

Differentiating random unrelated elements (accidental coincidences) from coupled elements relies on the creation of two models. The GW and sensor channels are analyzed individually to identify interesting artifacts (glitches). Properties like signal-to-noise ratio (SNR), frequency, duration and time of interest are recorded. By using these measured properties or any subset of these properties we can construct two artifact sets. The physically interesting set what we call the coupled model (foreground), describes the temporal relationship between the GW data output and activity in the instrument's environment. It also contains unrelated time coincidences (accidental coincidences), for this reason one needs a second set. This second set of artifacts is what we call the uncoupled model (background), which has randomly assigned relationships between elements in the GW and sensor data streams.

As the name implies the Critical Coupling Likelihood is a method which is capable of determining the likelihood of instrumental coupling being absent or present. The CCL method evaluates the potential for coupling at a specific time, between the GW channel and a individual sensor channel paired to it. For the GW channel, we apply a selection criteria to restrict the number of identified artifacts ( $y_i$ ) (i.e. frequency interval, SNR range, etc), and this set is defined as

$$\mathbf{Y} = [y_1, y_2, \dots, y_m]. \quad (1)$$

For the sensor channel we use all the artifacts ( $x_i$ ) identified without applying any particular selection criteria, and this set is defined as

$$\mathbf{X} = [x_1, x_2, \dots, x_n]. \quad (2)$$

The data will have inherent restrictions related its epoch of occurrence, due to operating conditions of the detector, reflecting the timescale of detector stationarity.

### 3. Sampling Method

The models need to be created from sufficiently sampled data to adequately describe potential relationships between the instrument and environmental effects. The epoch of sampling validity is defined as a time interval when only trivial changes to the running state of the GW detector have occurred because one expects the detector behavior to be nearly unchanged. In defining epochs this way, the unknown coupling function (system function) should be nearly stationary between the GW detector and environment [20]. The minimum amount of data required to build a reliable model is directly proportional to the rate of the sensor artifacts recorded and as such the total amount of aggregated time (samples) required to build each model will be sensor dependent.

There are two approaches for sampling the data that can be done for models construction. The first approach is to sample the GW data stream uniformly, requiring a minimum of number of samples per unit time,  $\phi$ . The alternate approach favored for the CCL tests is to sample the GW data stream using combined conditions. First, we impose a minimum overall sampling rate  $\phi_{\text{low}}$ . This ensures that samples are taken over the entire model epoch. We then impose a second condition on sample SNR  $\rho_0$ , which is  $\bar{\rho} \geq \bar{\rho}_{\text{low}}$ , using a running average on  $\rho$ . For periods of high  $\rho$  we increase  $\phi$  to a higher temporary sampling rate,  $\phi'$ . The sampling thresholds  $\phi_{\text{low}}$  and  $\rho_0$ , must be fixed for the entire sampling epoch used to construct the model. By using  $\phi$  and  $\rho$ , it is possible to determine a instantaneous sampling rate which favors sampling times of instrumental malfunction. We call this hierarchical sampling approach *targeted sampling*.

### 4. Model Resolution

The statistical properties of the collected data sets can be expressed by a probability mass function (PMF). Each model (coupled and uncoupled) is represented by a 2 dimensional (2D) conditional probability distribution (CPD) which associates SNRs in the GW channel and the sensor channel. The resolution of the CPD, is dependent on the observation epoch and the sensor channel paired with the GW channel. Due to the discrete nature of the data, the resolution of the CPDs and PMFs is finite.

In the GW and sensor data sets there will be an unknown number of distributions which contribute to the observed artifacts. It is assumed that real instruments should have a baseline noise component plus possibly an additional unknown number of distributions. The SNR of the artifacts due to the Gaussian noise component of the data is Rayleigh distributed [9], this is the baseline noise. These Rayleigh distributed artifacts are the largest contribution to the number of observed artifacts. Due to the large number of low SNR artifacts a minimum SNR threshold  $x_0$  is applied. The artifacts which are below  $x_0$  are assumed to be part of the inherent instrumental noise. This threshold should be a reasonably low value because it inadvertently censors the Rayleigh artifact distribution. The following equation expresses the resulting Rayleigh

distribution of SNRs as

$$R(x) = \begin{cases} \frac{x}{\sigma^2} e^{-\frac{x^2}{2\sigma^2}} & , x > x_0 \\ 0 & , x \leq x_0. \end{cases} \quad (3)$$

In addition to the Rayleigh noise artifacts observed in LIGO data there is also an excess of outlier artifacts. It is reasonable describe this excess as at least one additional distribution<sup>‡</sup>. In reviewing a variety of data sets we empirically determined that the most reasonable way to describe the observed high SNR outliers is a Modified Weibull Distribution [12]. The Weibull distribution varies slightly from the standard form and it is described as follows:

$$W(x|\alpha) = \begin{cases} \frac{k}{\lambda} \left( \frac{z(x)-\alpha}{\lambda} \right)^{k-1} e^{-\left( \frac{z(x)-\alpha}{\lambda} \right)^k} & , z(x) - \alpha > 0 \\ 0 & , z(x) - \alpha \leq 0 \end{cases} \quad (4)$$

where  $z(x) = \log(x)$ . The profile of such distribution is determined by three parameters: the shape parameter  $k$  where  $k > 0$ ; the scale parameter  $\lambda$  where  $\lambda > 0$ ; the shift parameter  $\alpha$  where  $\alpha \geq 0$ . The parameter  $\alpha$  sets the zero point of the Weibull distribution. A properly selected  $\alpha$  parameter allows us to combine the expected Rayleigh and Weibull distributions together as a *single* probability distribution. In some extreme cases, the dual distribution assumption will break down for some data sets. The method described in this paper is easily generalized to integrate additional  $W_i(x|\alpha_i)$  distributions to combat this occasional method breakdown, but this generalization can become computationally challenging [11].

We defined this custom probability distribution function (PDF)  $C(x|\alpha)$ , defining it as

$$C(x|\alpha) = \psi_1 R(x) + \psi_2 W(x|\alpha), \quad (5)$$

where  $\psi_i$  with  $i = 1, 2$  are scaling parameters denoting the amount of relative Rayleigh and Weibull based artifacts. The  $\psi$  values are expected to behave in such a way to satisfy

$$\int_{x_0}^{x_{\max}} C(x|\alpha) = 1 \quad (6)$$

and thus  $C(x|\alpha)$  is normalizable. Figure 1 is a sketch of  $C(x|\alpha)$ , showing the relationship between  $R(x)$  and  $W(x)$ .

The best fit should have the largest number of bins possible, while minimizing the number of empty bins. The data sets contain a large range of observed SNRs, as such, it is better discretize this data using logarithmically spaced bins rather than linearly spaced ones. Consider a set of bin edges which are base  $B$  logarithmically separated, the optimal choice of  $B$  can be determined by maximizing the total histogram entropy [13]. The choice of  $B$  can be done iteratively, so that the resulting histogram of the data can easily be fit to the Rayleigh portion (low SNR) and also to the Weibull portion (high SNR) of  $C(x|\alpha)$ . To achieve this we must compute the entropy of the histogram as a function of  $B$ , which we expect to be in the set  $[2 \dots 10)$ . One must also decide the number of bins  $b$  that should be used for histogram construction. In order to determine the best binning to use one would simultaneously maximize the

<sup>‡</sup> This second distribution is observed in LIGO data. It can not be explained by Gaussian processes. It is mostly due to instrumental malfunction and environmental causes.

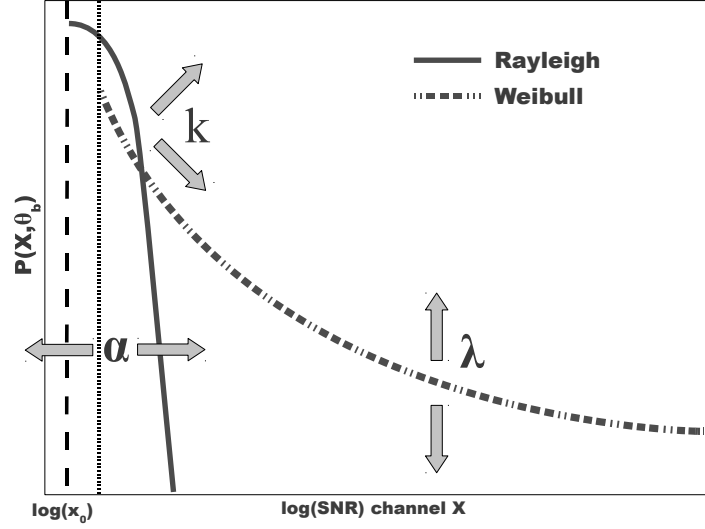


Figure 1: Background Model. We had determined empirically that background is composed of two distributions. These distributions are Rayleigh, followed by a second distribution. The second distribution is assumed to be a Modified Weibull distribution. Together these distributions form the background distribution of the CCL artifacts.

entropy of the histogram across both  $B$  and  $b$ . To discretely compute the entropy  $H(x, b, B)$ , we use the following expression,

$$H(x, b, B) = -\sum_{i=1}^b v_i(x) \ln v_i(x) \Delta x_i \quad (7)$$

with the following normalization

$$\sum_{i=1}^b v_i(x) \Delta x_i = 1. \quad (8)$$

The width scale of  $\Delta x_i$  is logarithmically increasing by  $B$ , and the value of  $v_i(x)$  is just the normalized element count in that bin. Optimizing the logarithmic scaling to the highest bin resolution possible is simply a matter of identifying the global maximum of  $H(x, b, B)$ . A maximum entropy representation of the data allows for the most suitable fitting of the distribution parameters possible.

#### 4.1. Fitting the underlying distributions

It is important that the underlying distributions the sampled data set fit well. Properly fitting  $C(x)$  PDF involves determining the parameters,  $\sigma$ ,  $\alpha$ ,  $\lambda$ ,  $k$ ,  $\psi_1, \psi_2$  while respecting the threshold  $x_0$ . To achieve this fitting we use one of two similar approaches. The choice of which approach to determine the parameters is a direct consequence of the data set size, and ability to properly histogram the sampled data. Under typical circumstances, the approach of choice would be Quantile Maximum Product of Spacing (QMPS). The QMPS works well if the data can be fit to a high entropy histogram, rich in data samples. In some cases the data sets are sparse and a high entropy histogram can not be created. For this situation we use a fitting approach

named Maximum Product of Spacing (MPS). The MPS approach uses all available data from the set and is inherently more tedious to apply than the QPMS approach. The two different approaches converge to the same parameters for data streams that are sufficiently sampled [14, 15].

The QPMS presented itself to be the most effective approach to determine the parameters of  $C(x)$ . The cumulative distribution function (CDF)  $c(\sigma, \alpha, k, \lambda, x_0, \psi_1, \psi_2|x)$  of  $C(x)$  is defined from the CDF of  $R(x)$

$$r(\sigma|x) = 1 - e^{-\left(\frac{x^2}{\sigma^2}\right)}, \quad (9)$$

and from the CDF of  $W(x|\alpha)$

$$w(\alpha, \lambda, k|x) = 1 - e^{-\left(\frac{z(x)-\alpha}{\lambda}\right)^k}, \quad (10)$$

and has the following form

$$c(\sigma, \alpha, k, \lambda, x_0, \psi_1, \psi_2|x) = \psi_1 + \psi_2 - \psi_1 e^{-\left(\frac{x^2}{\sigma^2}\right)} - \psi_2 e^{-\left(\frac{z(x)-\alpha}{\lambda}\right)^k}. \quad (11)$$

The parameters of interest are found by maximizing the quantity  $S(\sigma, \lambda, k, \alpha, \psi_1, \psi_2|\mathbf{X})$  using QPMS as follows,

$$S(\sigma, \lambda, k, \alpha, \psi_1, \psi_2|\mathbf{X}) = \prod_{i=0}^b \left( \psi_1 \left( -e^{-\left(\frac{-\hat{x}_i^2}{2\sigma^2}\right)} + e^{-\left(\frac{-\hat{x}_i^2-1}{2\sigma^2}\right)} \right) + \psi_2 \left( -e^{-\left(\frac{\hat{x}_i-\alpha}{\lambda}\right)^k} + e^{-\left(\frac{\hat{x}_i-1-\alpha}{\lambda}\right)^k} \right) \right)^{n_i} \quad (12)$$

all parameters can be fitted simultaneously. Where  $n_i$  is the element count for the  $i$ th bin, composed of  $\hat{x}_i$  elements. Using this method will give us all the fitting parameters required to characterize the sampled data.

In the case that data samples are sparse, MPS is used to determine the parameters of interest. The MPS also seeks to maximize the quantity  $S(\sigma, \lambda, k, \alpha, \psi_1, \psi_2|x)$ , but this approach varies slightly as follows

$$S(\sigma, \lambda, k, \alpha, \psi_1, \psi_2|\mathbf{x}) = \prod_{i=0}^j \left( \psi_1 \left( -e^{-\left(\frac{-x_i^2}{2\sigma^2}\right)} + e^{-\left(\frac{-x_i^2-1}{2\sigma^2}\right)} \right) + \psi_2 \left( -e^{-\left(\frac{x_i-\alpha}{\lambda}\right)^k} + e^{-\left(\frac{x_i-1-\alpha}{\lambda}\right)^k} \right) \right), \quad (13)$$

where the notable difference is that  $j$  is the total number of elements  $x_i$  used to fit the parameters simultaneously. Implementing this calculation for very large values of  $j$ , becomes computational slow, so one should use QPMS whenever possible.

## 5. Creating Coupled and Uncoupled Models

The artifact information which is used to construct the coupled model is derived by applying a time coincidence check. We define being coincident in time by using window,  $t_w$ , to compare events in both channels. The value of  $t_w$  is chosen empirically by comparing a large collection of sensor data streams with the GW data stream. When analyzing large sets of sensor channels, it is better to choose a  $t_w$  value which is long enough to capture all artifacts resulting from control loop delays, and physical

delays between an environmental influence and the expected GW detector response to this influence.

The coupled model data can be expressed as a conditional probability distribution (CPD) with the following form

$$P(\mathbf{Y}|\mathbf{X}, \theta_f) = \frac{P(\mathbf{Y} \cap \mathbf{X}, \theta_f)}{P(\mathbf{X}, \theta_f)} \quad (14)$$

where  $P(\mathbf{Y} \cap \mathbf{X}, \theta_f)$  is a two dimensional joint probability distribution (JPD). This JPD represents the probability of a element in the set  $Y$  (GW data), given set  $X$  (sensor data) for a specific model configuration  $\theta$ . In this expression  $\theta_f$  (foreground) denotes the set of samples drawn during potential coupling times and eventual applied constraints.

The data used to construct the uncoupled model is derived from all available  $\mathbf{X}$  and  $\mathbf{Y}$  artifacts. Unlike the coupled model, the uncoupled model is intentionally designed to break the statistical relationship between the elements of  $\mathbf{X}$  and  $\mathbf{Y}$ . Using the PDFs of  $\mathbf{X}$  and  $\mathbf{Y}$  we can build a background model JPD where we have forced statistical independence. This implies that the uncoupled model's JPD is simply

$$P(\mathbf{Y} \cap \mathbf{X}, \theta_b) = P(\mathbf{X}, \theta_b) \cdot P(\mathbf{Y}, \theta_b). \quad (15)$$

To ensure the uncoupled model's discrete CPD matches the resolution of the coupled model's CPD, the forms of  $P(\mathbf{X})$  and  $P(\mathbf{Y})$  must be reasonably well measured for the entire data set. In addition to knowing these two functions one must also expect that the data which represents the coupling in the coupled model is not the dominate source of data for constructing  $P(\mathbf{X})$  and  $P(\mathbf{Y})$ . This additional constraint is easily satisfied when building models between any one particular channel and the GW channel. In a real world application of the CCL algorithm, there should be no one preferred source of coupled artifacts in the GW channel produced by a single sensor input.

## 6. Calculation of CCL Function

The CCL function is defined as the log likelihood ratio between the coupled and uncoupled model previously described, and is given by

$$CCL(\mathbf{Y}, \mathbf{X}|\theta_f, \theta_b) = 2 \log_{10} \left( \frac{P(\mathbf{Y} \cap \mathbf{X}, \theta_f)}{P(\mathbf{Y} \cap \mathbf{X}, \theta_b)} \frac{P(\mathbf{X}, \theta_b)}{P(\mathbf{X}, \theta_f)} \right). \quad (16)$$

The above expression is easy to simply algebraically because of equation 15 yielding

$$CCL(\mathbf{Y}, \mathbf{X}|\theta_f, \theta_b) = 2 \log_{10} \left( \frac{P(\mathbf{Y} \cap \mathbf{X}, \theta_f)}{P(\mathbf{Y}, \theta_b)} \frac{1}{P(\mathbf{X}, \theta_f)} \right). \quad (17)$$

The CCL function quantifies the level of suspected coupling between a specific sensor and the GW data. The observed CCL value can be translated into one of three statements: no coupling suspected; coupling is suspected; or an indeterminate state where there is insufficient information to determine coupling. In the case of **No Coupling** the CCL values will be negative values indicating improbable coupling. For cases of **Coupling** the CCL values will be positive indicating an observed potential GW channel candidate is likely due to an localized noise source influencing the GW detector. When the values are close to zero, either positive or negative, the test is



incapable of determining if the GW candidate being tested is the result of coupling. There is no clear prescription for determining a single threshold on the CCL value that would be clearly indicative of coupling for all possible cases. In an optimal integration of the CCL method with a search the CCL values could be used to re-weight the significance of candidates, leaving the significance unchanged when the candidate can not be associated with any local observatory effects.

Visualizing the CCL function offers insight into the characteristics of the data. When we visualized preliminary functions we encountered distinct patterns in the CCL values as a function of SNR between the two data sets. One would expect there to be some sort of pattern visible in the functions, we found these patterns tend to be distinct. The distinctness of the patterns is attributable to the coupling mechanism described by the artifact distributions used to construct CCL models (foreground and background).

### 6.1. Visualizing and Interpreting CCL Function

There can be distinct features in a CCL function plot whose structure characterizes the observed relationship between coincident data in the GW channel and the sensor channel. We present on figure 2 an illustration of a few key regions which could be the result of potential coupling mechanisms. A CCL plot can be simply represented as a two dimensional color map. This color map has a pair of axis, one being the GW data,  $P(\mathbf{Y})$  and the other axis is the sensor data,  $P(\mathbf{X})$ .

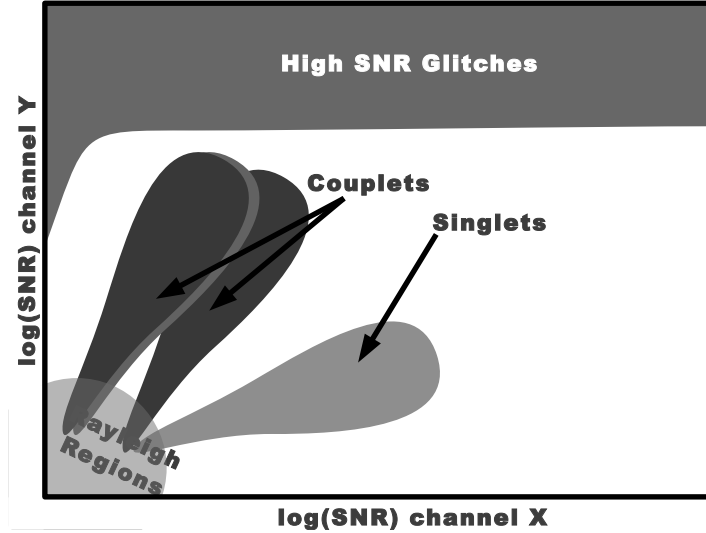


Figure 2: This figure outlines distinct regions and typical shapes that can be found in CCL functions. Different shaded regions correspond to different coupling patterns or inherent artifact properties of either the sensor or gravitational wave data.

The color map represents the CCL values calculated for the data set. All CCL functions will have a triangular-like region, *Rayleigh Noise*, composed of three joined regions, one circular and two triangular in shape (figure 2). All artifacts appearing

in this region must be assumed to be related to Gaussian fluctuations in either the sensor or the GW channels. There is no way to distinguish Rayleigh artifacts, which are not coupled, from potentially coupled artifacts, which can lay in one of the two smaller triangular regions. The Rayleigh regions are inherent to all CCL functions and are always present in some form in all the models.

For CCL functions which are indicative of coupling, the coupling mechanism will manifest itself as some type of structure. Figure 2, shows the four common structures observed in the sampled data. The specific area and shape of a region denotes the relationship between the data collected from the sensor and how the GW data stream is or is not affected by phenomena measured by the sensor.

The first region of interest is the *Singlet* region. Here the CCL values show what appears to be a quasi-linear relationship in a log-log space of observed artifact's SNR in the sensor data compared with the artifacts in the GW data. The second region of interest is *Couplets* and this structure is normally seen in pairs of CCL functions. Consider two sensor channels that see similar but not identical physical phenomena, like accelerometers and seismometers. Excessive ground motion at the observatory might produce similarly distributed artifacts in both channels and CCL function plots will show overlapping parallel structures. The last region observed in most CCL functions, which is not sharply defined, is the *High SNR Glitches* region. The events that compose this region are at the edge of linear behavior for differential arm motion sensing. Because of the potential for a non-linear instrument response, this region presents itself as unreliable [21].

These plots are useful as supplementary tools to visualize and help understand the relationships between the sensors and the detector output.

## 6.2. Disregarding CCL functions sensitive to gravitational waves

The observatory should in principle have its output, the gravitational wave data, as the only data stream which is sensitive to GWs. In practice this is not guaranteed to be the case. The observatory may have sensors which respond to the presence of a GW. It is unwise and not safe to use a CCL function derived from sensors which may be responding to passing GWs. One needs a prescription for identifying sensor channels that are unsafe so those functions will not be used to identify non-GW artifacts in the detector output [7, 8].

An unsafe CCL function, which could have undesirable sensitivity to GW phenomena, can be identified with a simple prescription. If the CCL function is unsafe the distribution of hardware injections identified by the function will be similar to the distribution of all hardware injection artifacts used to test the detector. As a result of this expectation identifying unsafe CCL functions can be accomplished by applying a Kolmogorov-Smirnov (KS) test. The null hypothesis would be, "For a given sensor  $S$ , is the distribution of the hardware injection artifacts identified with ( $\text{CCL} \geq 1$ ) the same as the distribution of all known hardware injection artifacts?". A CCL function is unsafe when

$$\sqrt{\frac{mn}{m+n}} \sup_x |F_{\theta_{f_{\text{hw}};m}}(x) - F_{\text{all}_{\text{hw}};n}(x)| \geq \kappa_\alpha, \quad (18)$$

with

$$F_a(x) = \frac{1}{a} \sum_{i=1}^a \begin{cases} 1 & \text{if } x_i < x \\ 0 & \text{if } x_i \geq x \end{cases}, \quad (19)$$

where  $F_{\theta_{f\text{hw};m}}(x)$  is the set of all hardware injection artifacts identified satisfying  $CCL \geq 1$  and  $F_{\text{allhw};n}(x)$  are all known hardware injection artifacts. The significance level  $\kappa_\alpha$  for this preliminary study was chosen to correspond to a confidence level of 0.85. The KS test will indicate if a CCL function is potentially preferentially selecting artifacts that are more like hardware injection artifacts, which implies that the CCL function would be sensitive to GW phenomena and thus shouldn't be used to identify coupling between the observatory and the environment.

## 7. Preliminary Results

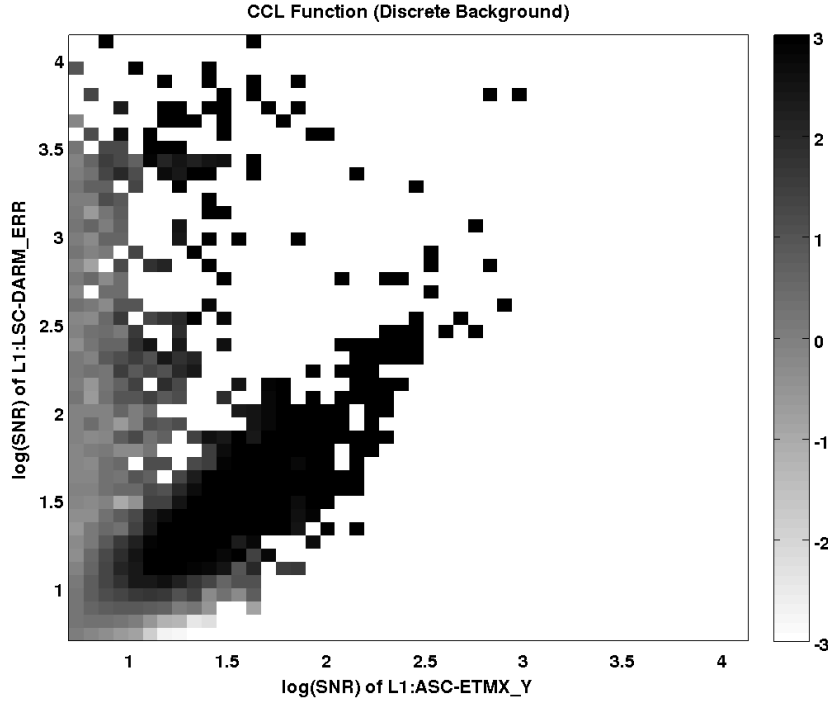
We will show how the Critical Coupling Likelihood (CCL) method responds to artifacts in LIGO data, while ignoring effects that can be attributed to potential GW signals. The data used in this analysis is a small sample of data totaling 3.5 days of observing data, derived from sampling a few months near the end of S6 for LIGO Livingston and LIGO Hanford observatories. The results presented here are intended to highlight typical CCL functions, and encouraging results derived from a limited set of input sensors.

The outputs of a CCL analysis are intended to make quantitative statements about the relationship of the instrument behavior relative to the studied sensor data. This is a single quantitative value, which is useful to determine the coupling state of the observatory. The functions which are used to compute a family of values quantifying the environmental state of the observatory are themselves useful to understand the physical coupling mechanisms which are identified by the CCL method. The CCL method has different behavior when applied to LIGO Livingston in comparison with LIGO Hanford. This difference in behavior is expected to be attributed to the distinctly different environments they operate in.

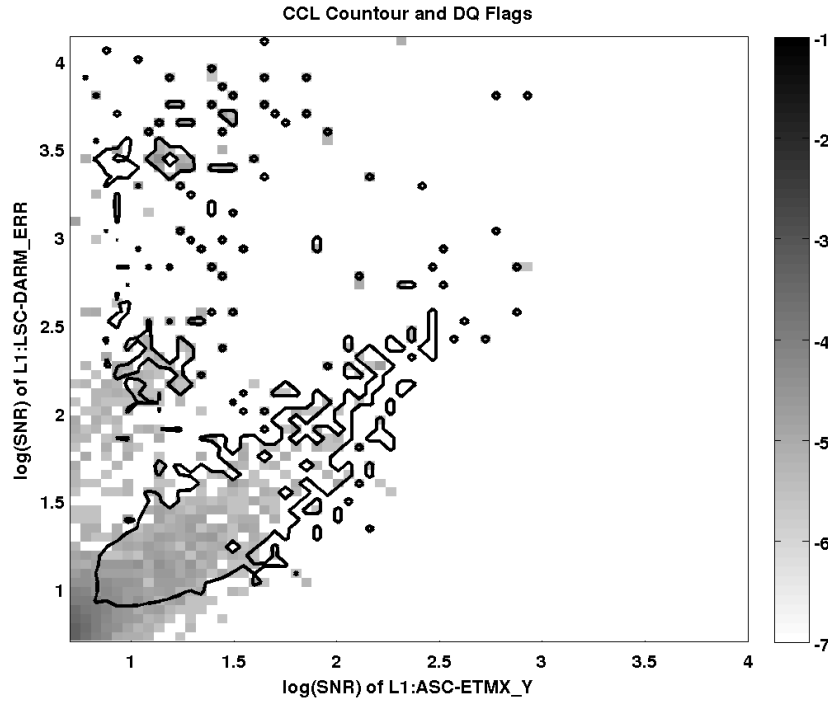
As an example, one of the many CCL functions generated for LIGO Livingston is plotted in figure 3a. In this plot there is identifiable structure, which is an example of a *Singlet*. The singlet in this function is indicative of coupling to the instrument through seismic motion, which is inducing pitch motion of LIGO's x-end test mass. It is reasonable to expect increasing pitch motion of the test mass to correspond to increasing SNR of artifacts in the GW detector output. This relationship is readily seen in the figure as an angled structure of high CCL values.

An example of a LIGO Hanford CCL function is shown in figures 4a and 5a. These figures have a different type of identifiable structure, a "Couplet". For CCL functions with this type of structure, the artifacts identified by this model are typically in common with another sensor. In both figures, there appears to be two singlet structures, where one singlet is better defined than the other. In figure 4a, the well defined singlet in that couplet structure corresponds to a poorly defined singlet structure in figure 5a. This relationship is reciprocal, the well defined singlet associated with the couplet in figure 5a is the poorly defined singlet associated with the couplet from figure 4a. The couplet structure appears in pairs of CCL functions. These pairs are usually related by obvious mechanisms as in demodulated signals or signals derived from mechanically interdependent systems. For these example figures, the two functions are witnessing artifacts which are partially encoded as an in-phase and quadrature components of light received by the same photo-diode assembly.

The CCL method can provide a metric to determine coupling into the observatory data. This metric is useful to understand if and what local environmental effects may be responsible for a false GW event. To appreciate the potential usefulness of a

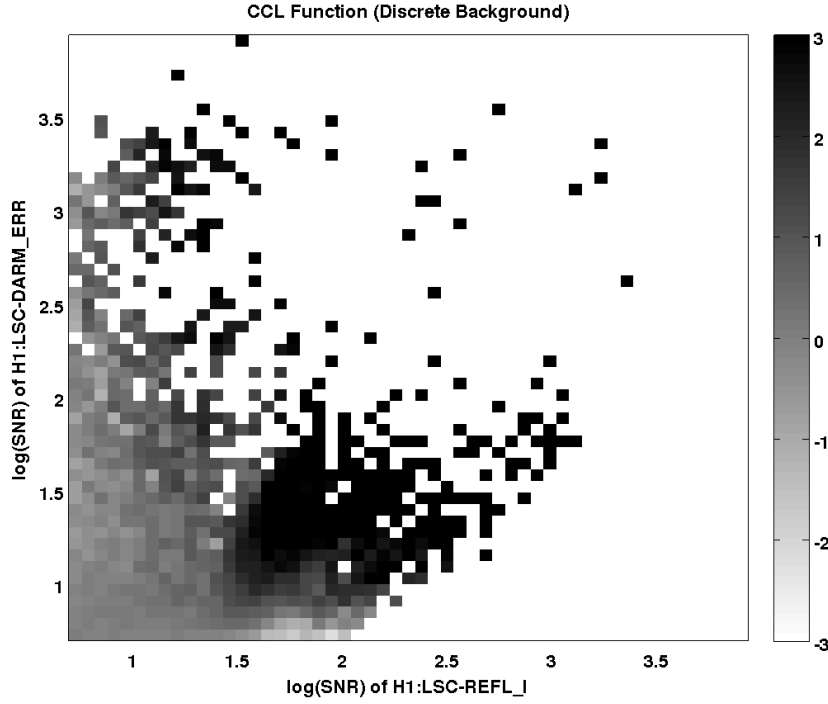


(a) CCL Function LLO (Singlet)

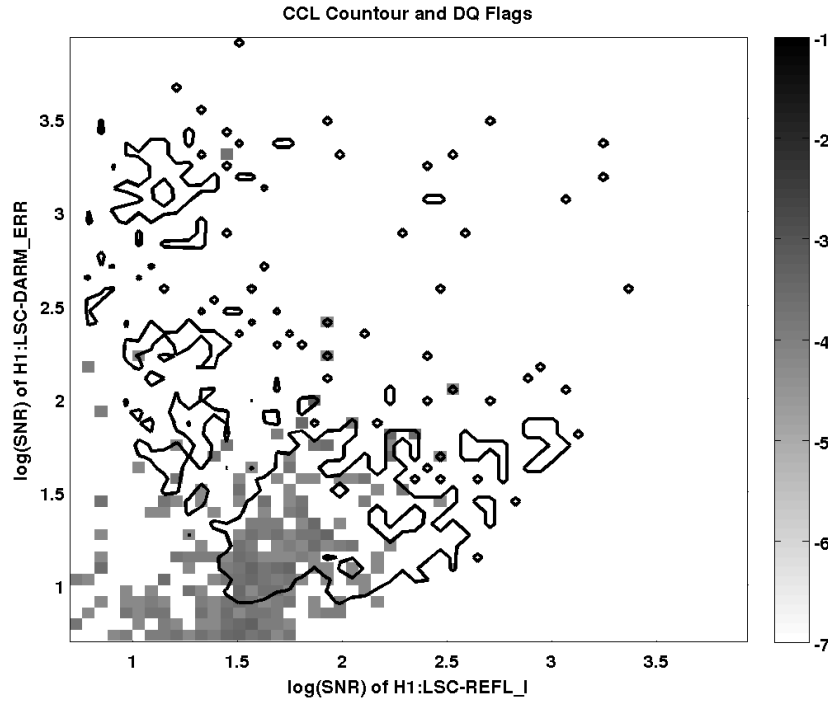


(b) CCL Function Contour includes DQ flags

Figure 3: In 3a we have an example “Singlet” structure, which shows linear correlation between artifacts in the sensor resulting in artifacts in the GW artifacts. In 3b the same information as show as a contour plot overlaid with artifacts identified using standard data quality approaches. One can notice that there is significant agreement between them.

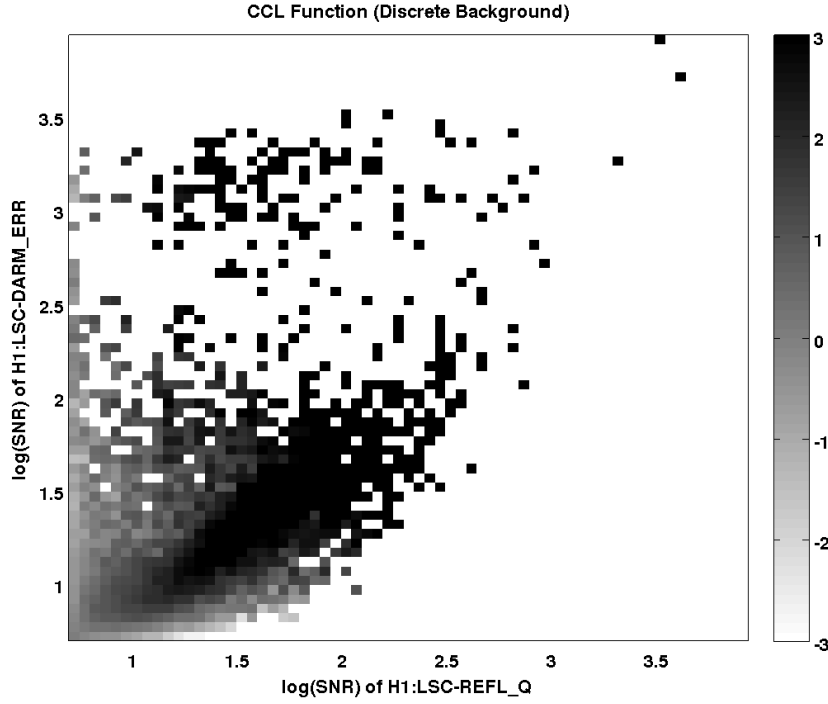


(a) CCL Function (Couplet)

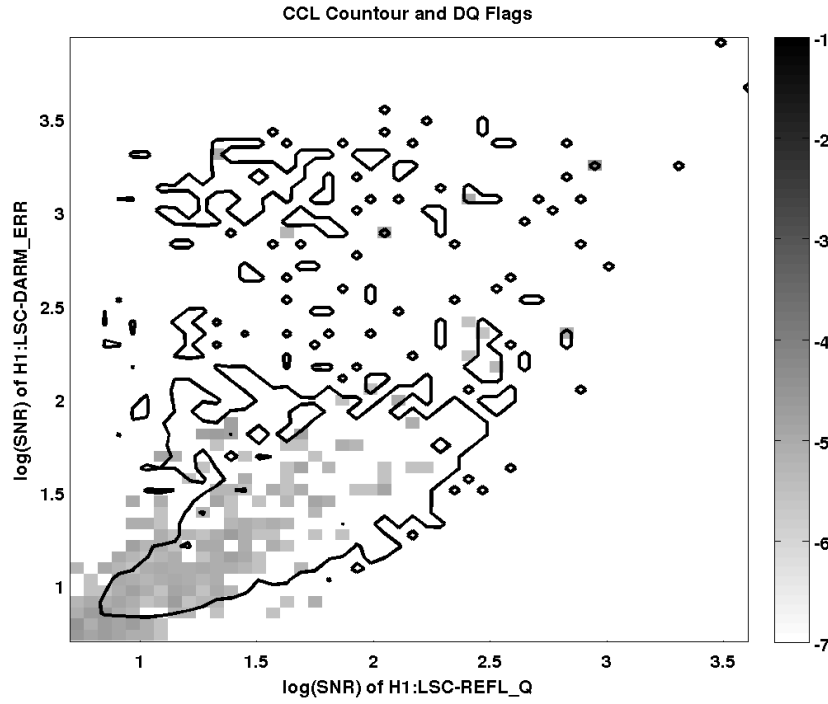


(b) CCL Function Contour includes DQ flags

Figure 4: In 4a we have an example “Couplet” structure, which shows bi-modal correlation between artifacts in the sensor resulting in artifacts in the GW artifacts. In 4b the CCL information is shown as a contour plot overlaid with artifacts identified using standard data quality approaches. In the contour plot the standard techniques show agreement for one half of the bi-modal region. The other half is identified in figure 5b.



(a) CCL Function(Couplet)



(b) CCL Function Contour includes DQ flags

Figure 5: In 5a we have an example part of the “Couplet” structure shown in figure 4a. In 5b the CCL information is shown as a contour plot overlaid with artifacts identified using standard data quality approaches. In the contour plot the standard techniques show agreement for one half of the bi-modal region. The other half is identified in figure 4b.

	Livingston	Hanford
Deadtime	13.9%	15.1%
SNR( $\geq$ )	%	%
5	14.4	16.3
8	82.3	93.5
10	88.8	96.7
20	86.7	98.0
50	92.4	98.9
100	98.0	99.2

Table 1: This is the efficiency and deadtime table for the Livingston and Hanford observatories. The deadtime estimated presented here is expected to be an upper limit on the expected deadtime for ( $\mathbf{CCL} \geq 1$ ).

method like the CCL method, we imposed a CCL threshold value, which declares an event as coupled about this value. By using a CCL cutoff,  $CCL \geq 1$ , it allows us to sort the identified artifacts into two groups inherent noise artifacts (uncoupled) and those which are due to environmental influences (coupled). This cutoff in CCL value corresponds to an identified artifact to be at least  $\sqrt{10}$  times more likely to be coupled than uncoupled, as defined in section 6. For LIGO Livingston, a total of **205** functions were used to identify the coupled artifacts. For LIGO Hanford, we used a total of **207** functions to identify the coupled artifacts in the Hanford data set. The set of artifacts that were analyzed is constructed by sampling Livingston and Hanford data with an average sampling rate of 1 sample every two minutes using only science mode times, where science mode times are times that are considered of high enough quality to perform a search for GW signals. Using this sampling constraint, the data set is less than 5 percent of the total amount of data available from the end of the last science run. We expect that if a more detailed sampling is performed over the same interval of observing time the results of our preliminary analysis will remain relatively unchanged. Using these constraints on sampling rate and sensors used, figures 6 and 7 shows the number of artifacts not identified as coupling after applying a hard CCL cut. For both figures, there is a clear suppression of the original outlier tails. What may not be readily apparent in these figures is that the CCL method appears able to suppress the outlier tail and identify moderate SNR artifacts, while leaving the original low SNR artifact distribution unchanged. In table 1, it is easier to see why one can appreciate the CCL method for identifying artifacts, because this method ignores SNR regions where artifacts tend to be the result of inherent properties of the instrument and likely not due to environmental influences. GW searches should have a net gain in sensitivity because the distribution of outlier artifacts are being suppressed by using CCL to identify artifacts suspected to be the result of environmental influences.

The sensor channels used in this preliminary study were those used as part of the standard followup activities done at the end of a GW search [5]. Using the safety prescription outlined in section 6.2 we discarded several channels suspected of presenting an undesirable sensitivity to GW phenomena and deemed to be potentially *unsafe*. According to such criteria, we were required to remove **10** functions for LIGO Hanford, and **9** functions for LIGO Livingston.

One can see in table 2, that the remaining *safe* channels identify a small fraction of the total number of hardware injection artifacts. There is a clear contrast between

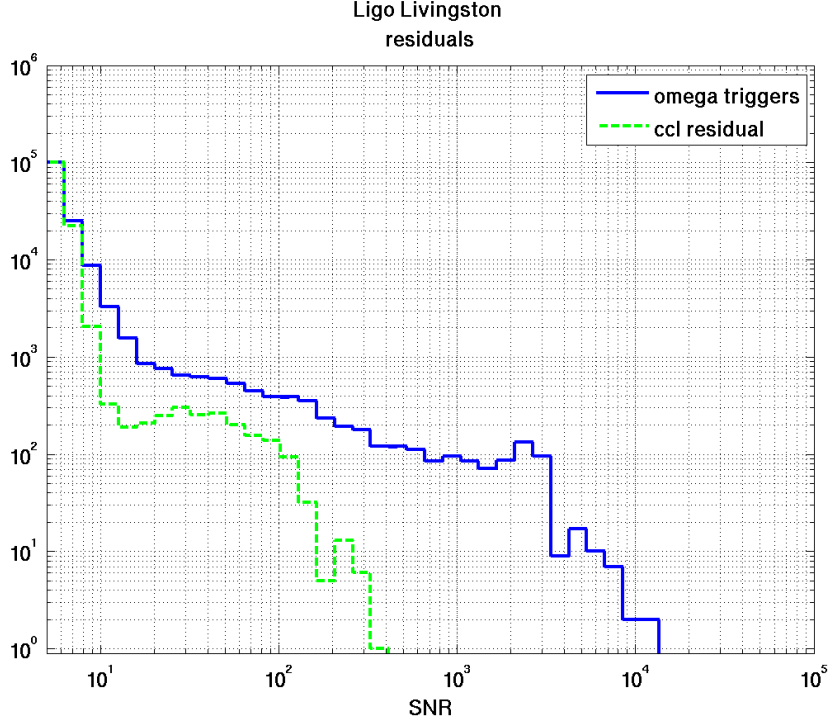


Figure 6: This figure shows the distribution of a sample set of LIGO Livingston GW artifacts, as a solid curve. The dotted curve is set of remaining artifacts from the sampled set (solid curve) after removing ( $CCL \geq 1$ ) identified artifacts.

Safe CCL Function Properties		
	Livingston	Hanford
Median Injection Count Per Function	2	4
Mean Injection Count Per Function	2.7(1.04%)	4.7(1.54%)
Standard Deviation on Count Per Function	2.3(0.87%)	4.2(1.39%)
Hardware injection artifacts in data set	265	303
Total Number of Functions	205	207

Table 2: This table shows the average hardware injection artifacts identified per CCL function. The distribution of hardware injection artifacts throughout all the CCL functions summarized here are quasi-uniform implying that such identifications were purely accidental.

the *safe* and *unsafe* functions, because one can see from tables 2 and 3 that the average number of hardware injections identified per CCL function for *safe* functions is less than 1.



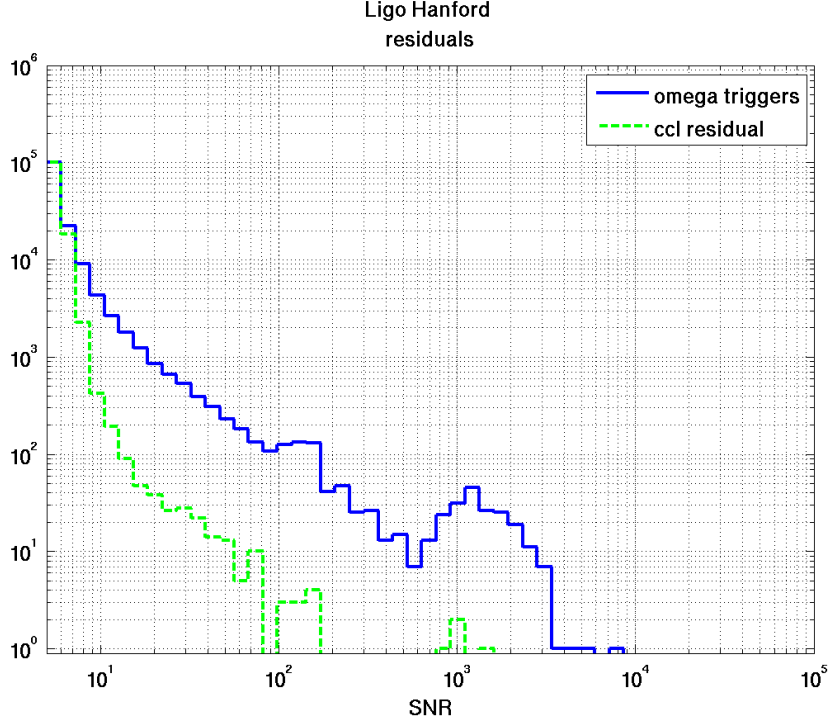


Figure 7: This figure shows the distribution of a sample set of LIGO Hanford GW artifacts, as a solid curve. The dotted curve is set of remaining artifacts from the sampled set (solid curve) after removing ( $CCL \geq 1$ ) identified artifacts.

Unsafe CCL Function Properties		
	Livingston	Hanford
Median Injection Count Per Function	7	9
Mean Injection Count Per Function	6.8(2.58%)	9.2(3.04%)
Standard Deviation on Count Per Function	1.2(0.47%)	3.1(1.05%)
Hardware injection artifacts in data set	265	303
Total Number of Functions	9	10

Table 3: This table shows the average hardware injection artifacts identified per CCL function. The distribution of hardware injection artifacts throughout all these CCL functions were consistent with the distribution of hardware injection artifacts. This consistency implies that these channels are potentially sensitive to GW phenomena and are unsafe in identifying environmental coupling.

## 8. Conclusions and Future Directions

The Critical Coupling Likelihood method is intended to improve future gravitational wave search efficiency and provide feedback to instrument scientists at the observatory. The results shown here are preliminary and are produced using a small set of LIGO data. We expect to see this same level of performance if we apply this approach to a full set of existing LIGO data or future aLIGO data. This method is very promising because it offers quantified observatory information which can be directly imported into a GW search. In creating this quantified observatory information, the CCL method is also providing instrument scientists with information that describes potential coupling mechanisms between the instruments operating environment and the instruments behavior. Using this method as part of analysis or as a tool to directly investigate instrument behavior, one can expect the CCL method to help improve the quality of the data generated.

In this paper we introduced a new detector characterization technique called the Critical Coupling Likelihood method. This method is intended to use all available observatory information and deduce the presence of coupling between the environment and the detector. In making this coupling identification it also implicitly estimates the coupling relationship giving information about how the strength of local environmental effects map into specific noise levels and frequency bands. These preliminary results presented in the paper indicate that an approach like CCL should have an appreciable impact on the effectiveness of future GW searches, by reducing the outlier tail. Our initial results show CCL identifying  $\sim 80\%$  of observed artifacts with  $SNR \geq 8$ . Identifying these outlier events lead to significant outlier tail suppression which is clearly seen in figures 6 and 7. By using this technique we can quantitatively characterize individual GW candidates, accounting for instrumental conditions, and hence improve GW searches and the validation of a detection.

## 9. Acknowledgments

The authors gratefully acknowledge the support of the United States National Science Foundation for the construction and operation of the LIGO Laboratory. The authors also thank LIGO and the LIGO Scientific Collaboration for allowing the use of LIGO data for this study. The authors would also like to acknowledge the support of this research via NSF grants PHY-0905184 and PHY-0757058. This paper was assigned LIGO document number LIGO-P1000187.

## References

- [1] <http://www.ligo.org>
- [2] G. Harry *et al.* **Class. Quantum Grav.**, 27, 084006, 2010.
- [3] J. Abadie *et al.* **Class. Quantum Grav.**, 27, 173001, 2010.
- [4] I. Mandel *et al.* **ApJ**, 681, 1431, 2008.
- [5] C. V. Torres and R. Gouaty. *The Compact Binary Coalescence Search Follow-up the Home Stretch*, 2010 International School on Numerical Relativity and Gravitational Waves, Asia Pacific Center for Theoretical Physics, Pohang Korea , LIGO-G1000679
- [6] B. Abbott *et al.* **Phys. Rev. D**, 79, 122001, 2009.
- [7] N Leroy *et al.* **2009 Class. Quantum Grav.** 26 204007
- [8] J Slutsky *et al.* **2010 Class. Quantum Grav.** 27 165023
- [9] N. Christensen *et al.* **Class. Quantum Grav.**, 27, 194010, 2010.
- [10] B. Abbott *et al.* **Phys. Rev. D**, 80, 102001, 2009.

- [11] J. Hernandez and I. Phillips. **IEE Proc. Commun.**, 153, 2, 2006.
- [12] W. Nelson. *Applied Life Data Analysis*. Wiley-Interscience, 2003.
- [13] R. Collins and A. Wragg. **J. Phys. A:Math. Gen.**, Vol. 10, No. 9, 1977
- [14] R. Cheng and N. Amin. **J. R. Stat. Soc. Ser. B Stat. Methodol.**, 45(3), 394, 1983.
- [15] D. Cousineau. **IEEE Trans. on Dielect. and Elect. Ins.**, 16(1), 281, 2009.
- [16] B. Abbott *et al.* **Rep. Prog. Phys.**, 72, 076901.
- [17] V. Majernik, **Rep. Math Phys.**, Vol. 45 No. 2 (2000)
- [18] A. Abbas, **IEEE T Eng Manage** , Vol. 53 No. 1 (2006)
- [19] Sheskin D., **Handbook of parametric and nonparametric statistical procedures** 4th ed. Chapman & Hall 2007
- [20] R. McDonough and A. Whalen, **Detection of Signals in Noise**, Academic Press (1995)
- [21] J. Abadie **NUCL INSTRUM METH A**, Vol. 624 p223 (2010)